13.6 AIRBORNE RADAR OBSERVATIONS OF BREAKING WAVES/ROTORS IN THE LEE OF THE MEDICINE BOW MOUNTAINS IN SE WYOMING, USA

Jeffrey R. French[1]*, Samuel Haimov[1], Larry Oolman[1], Vanda Grubišić[2], and Dave Leon[1]
[1]University of Wyoming, Laramie, WY
[2]Desert Research Institute, Reno, NV

1. INTRODUCTION

Rotors are horizontally aligned vortices that form in flow downstream of terrain barriers such as mountain ranges. The fundamental physics of the coupled wave-rotor system is not fully understood, due in large part to the dangerous nature of obtaining measurements within these systems. Recent advances in remote sensing technology specifically airborne Doppler radars and lidars, have made it possible to obtain observations of the interior of rotors. These high resolution measurements offer a new avenue to study severe atmospheric turbulent phenomena such as rotor/wave systems as well as components of these systems such as sub-rotor structures.

In January/February 2006, the University of Wyoming King Air (UWKA) research aircraft, instrumented with the Wyoming Cloud Radar (WCR), conducted a field campaign over the Medicine Bow Mountains in SE Wyoming. One of the campaign's objectives was to investigate the formation of orographic precipitation as air passed up and over the mountain barrier. The data collected through repeated passes of the aircraft along the wind and across the barrier was also well suited to investigate the formation of waves.

In this paper we present analyses of data collected on two days during this campaign. A companion paper (Oolman et al., 2008, this conference) presents analyses of the basic meteorological conditions on these days. Here we present detailed observations of the wave/rotor systems. In section 2 we discuss the data and collection, in section 3, the observations and interpretation, and in section 4 we summarize our findings and discuss future work.

2. DATA

The data presented herein were collected from the University of Wyoming King Air research aircraft (UWKA, http://www.atmos.uwyo.edu/n2uw). We analyze measurements from two cases, 26 Jan and 5 Feb during the NASA06 field campaign in SE Wyoming (see acknowledgements). In situ measurements of the three-dimensional wind vector and other state parameters are provided by probes mounted on UWKA. In addition, remotely sensed measures of radar reflectivity factor and Doppler particle velocity are provided by the Wyoming Cloud Radar (WCR) also mounted on the UWKA (http://www.atmos.uwyo.edu/wcr).

The WCR is a 95 GHz (W-band) radar capable of measuring microphysical properties and Doppler velocity from up to 4 fixed antennas simultaneously from the UWKA. The data presented in the present study were collected from three of the beams, one pointed vertically upward, another pointed vertically downward (nadir) and a third pointed roughly 30 degree forward of nadir. Doppler velocity measurements from the two downward pointing antennas are combined to retrieve a two-dimensional cross-section of the velocity field along the vertical plane (curtain) swept by the beams (Leon and Vali, 2006). Details of the algorithm and discussion of uncertainties and errors for the method used in this study are given by Damiani and Haimov (2006).

The WCR is very sensitive to scattering by ice crystals. Radar measurements during the NASA06 campaign were aided by this since the campaign took place in winter time and in a region where most or all of the clouds are composed of ice crystals and aggregates. Further, because the ground was snow covered, strong winds near the surface could loft snow crystals and provide scatterers in regions that would have been otherwise devoid of scatterers.

The single-Doppler and dual-Doppler analyses presented in the following sections have been corrected for aircraft motion. Also, since the radar measures the velocity of particles, there is some uncertainty introduced due to inertia and fallspeed of the particles. Herein, we ignore the contribution of error due to particle inertia, and we further assume the contribution to the vertical component of the Doppler velocity due to particle fallspeed is on the order of 1 m s^{-1}. This resultant 1 m s^{-1} bias

* *Corresponding author address:* Jeffrey R. French, Dept. Atmospheric Science, University of Wyoming, Laramie, WY 82072; *email:* jfrench@uwyo.edu

in the measurements has been removed such that the radar velocities presented best represent the air motion.

3. Observations

The Medicine Bow Mountains of SE Wyoming are a dome-shaped range with a slight elongation in the SSW to NNE direction. The highest peak rises 1000 m above the surrounding terrain. As part of the NASA06 campaign, the UWKA flew repeated legs at altitudes as low as 700 m above the highest terrain. The flight legs were flown along the mean wind direction at flight level. This was generally within 10-15 degrees of the mean wind direction near ground level, based on aircraft soundings and measurements of wind direction at airports upwind and downwind of the mountain barrier.

3.1 26 January Case

On 26 Jan, the UWKA made three passes at 5000 m MSL over a period of 37 minutes, sampling a mountain cap cloud and a gravity wave that formed over the lee-side valley. The first and third pass were flown upstream to downstream with respect to the wind, within a km of each other. The second pass was flown in the opposite direction (upstream) offset by more than 3 km to the south. Figure 1 shows reflectivity measured from the WCR above and below the aircraft for the first and third pass. During both passes, observed winds at flight level were in excess of 20 m s^{-1} and peak vertical winds encountered by the aircraft (at the location of the wave crest) were greater than 12 m s^{-1}.

From the image, it is evident that cloud formed on the upslope side of the mountain. The slope of the cloud top, assuming a 20 m s^{-1} horizontal wind, is consistent with ice crystals falling at 1 m s^{-1}. The strongest echoes occur near ground level at or just downstream of the highest terrain. A layer of strong echoes extends downstream of here within 0.5 km of the ground. These echoes are consistent with falling and/or blowing snow down the leeward slope of the mountain.

Both the radar data and measurements from the aircraft suggest the primary wave formed 20 km downstream of the highest terrain (see arrows in figure 1) with a wavelength of 8 to 10 km. The wave propagated upstream, approximately 6 km over the 35 minutes between the first and third passes.

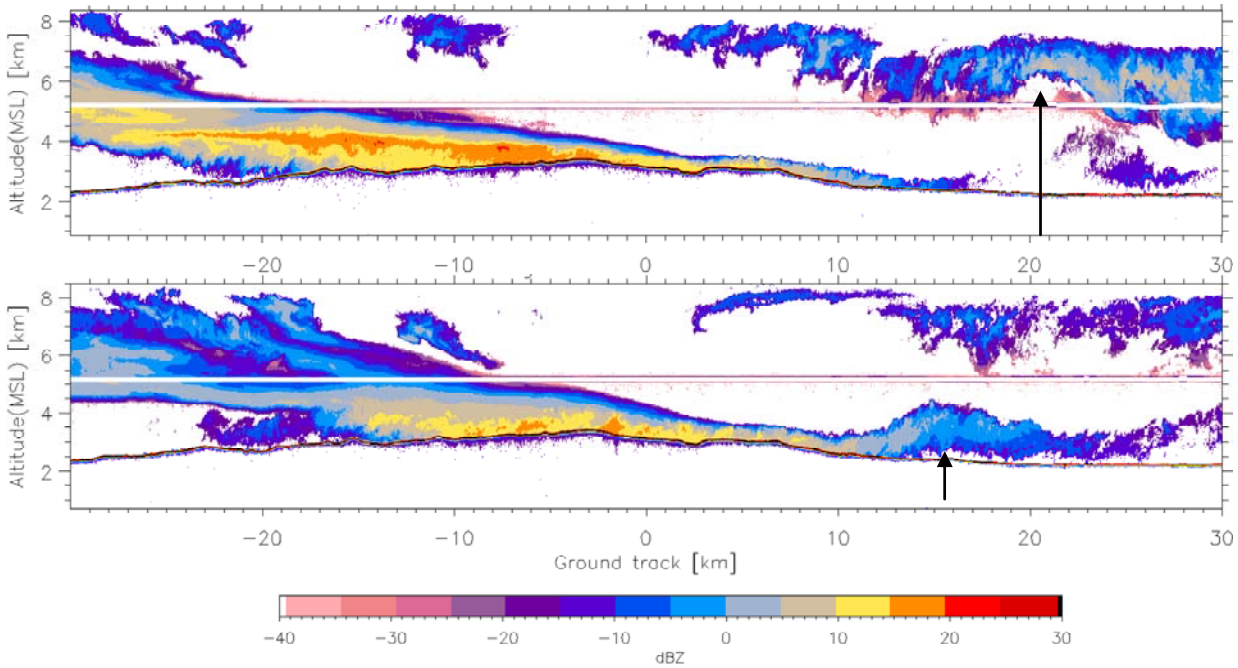

Figure 1: Reflectivity from the first (top) and third (bottom) pass on 26 Jan. The white line indicates the flight level of the UWKA. The origin is located just east of the highest terrain. The wind is from left to right. The crest of the wave (location of arrow) is apparent in the image above the aircraft at around 21 km on the first pass and below the aircraft further upstream at around 16 km on the third pass.

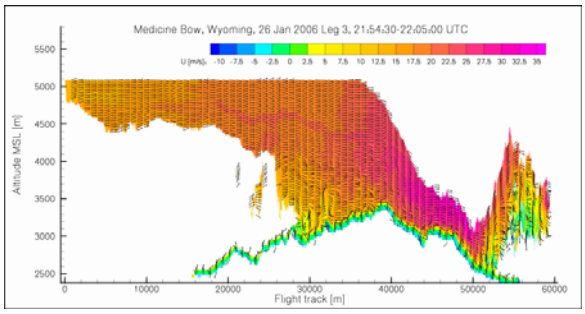

Figure 2: Vectors indicating two-dimensional flow field derived from dual-Doppler synthesis for data collected during the third pass. The color scale corresponds to the magnitude of the derived horizontal wind.

Figure 3: View from the forward video during the third pass.

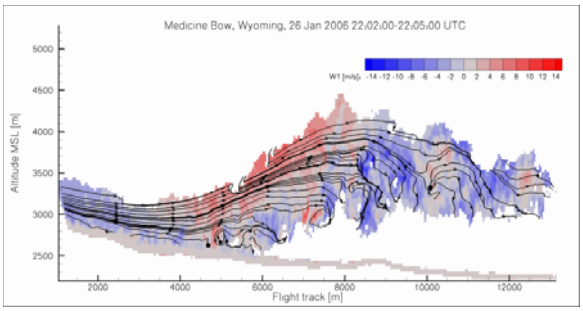

Figure 4: Streamlines derived from dual-Doppler synthesis during the third pass. The color scale corresponds to the vertical motion, red indicates upward moving air.

The strongest updrafts (>12 m s^{-1}) at flight level were encountered during the first pass. At this time, there was insufficient signal below the aircraft to complete a dual-Doppler synthesis for the region within the wave. By the third pass, those scatterers being carried down the lee-slope of the mountain extended far enough downstream to have been ingested into the wave. This allowed for a more detailed analysis of the radar data.

Figure 2 shows results from a dual-Doppler synthesis from data collected during the third pass. The color scale in the figure corresponds to the magnitude of the horizontal wind. At this time, the strongest winds were located downwind of the mountain crest a few hundred meters above the ground as the air accelerated down the lee-side of the slope. Winds in excess of 30 m s^{-1} were recorded. Near the valley floor, evidence from the radar indicates a separation of flow from the underlying terrain. Indeed at this time, there existed visual evidence of a roll cloud (see Figure 3).

Figure 4 shows streamlines from the same dual-Doppler synthesis shown in Figure 2 zoomed to the spatial scale of the rotor. In this figure the color scale corresponds to the retrieved vertical velocity field. The flow field is relatively smooth through the updraft region of the wave, at the point of flow separation from the surface. Numerous eddies, or sub-rotors, are evident nearer to ground level. These features are of size on the order of hundreds of meters or less, and are readily identifiable in the computed horizontal vorticity field (Figure 5). From the wave crest and further downstream, the flow becomes much more turbulent. This is evident from flight level data as well (not shown).

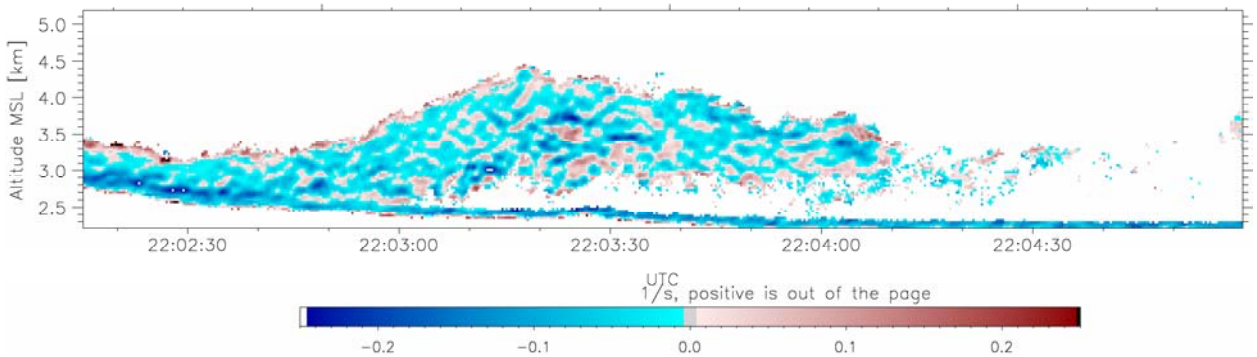

Figure 5: Computed horizontal vorticity field from dual-Doppler synthesis for data collected during the third pass. Sign convention is positive coming out of the figure.

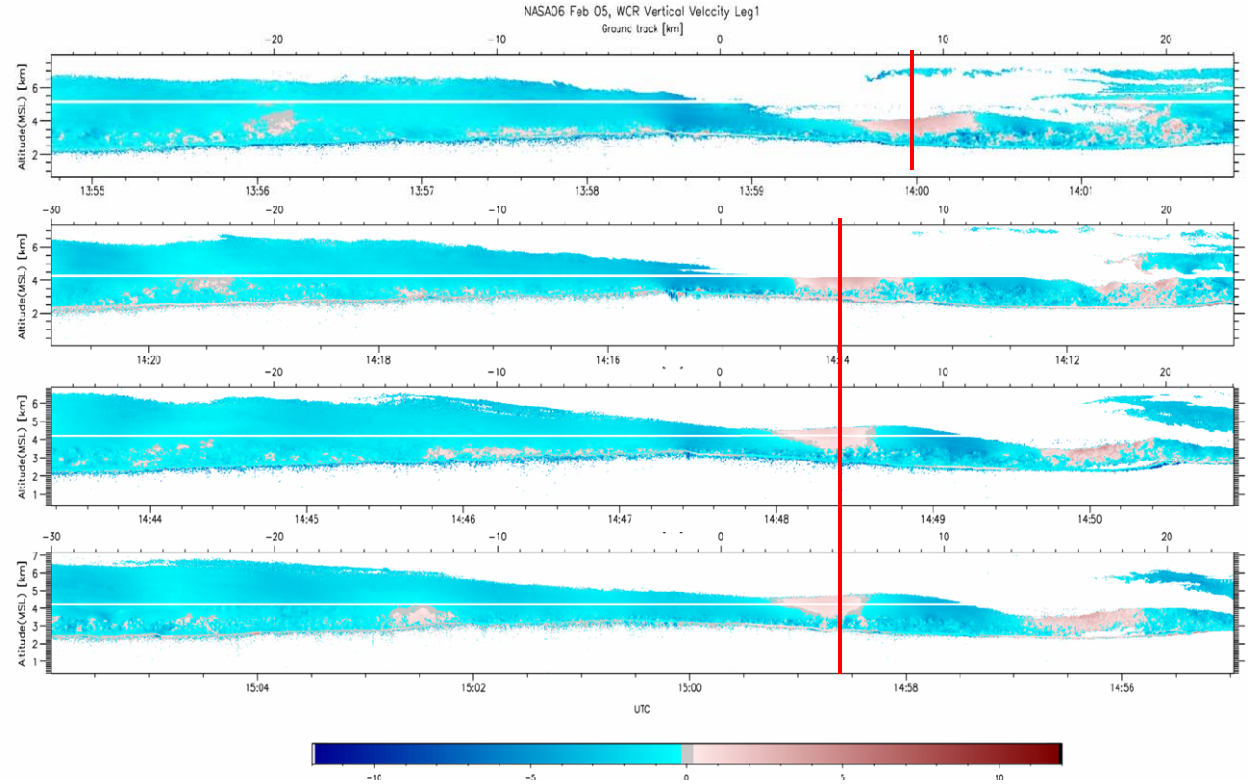

Figure 6: Vertical velocity from the WCR measured during the 4 passes on 5 February. The red line indicates the horizontal location of the primary wave crest based on the radar measurements. These locations match with in situ measurements provided by the UWKA.

3.1 5 February Case

On 5 February, the UWKA made four passes through a mountain cap cloud and wave train over a period of 1 hour. The first pass was made at 5000 m MSL, and the next three at approximately 4200 m MSL (700 m above the highest terrain). All four of the passes were flown within 1 km of each, oriented along the wind direction at flight level.

The wave train encountered over the period of all four passes was remarkably stationary. The train consisted of at least 2-3 full wave cycles with wavelength of approximately 12 km (see Figure 6). Maximum vertical winds encountered by the UWKA and measured by the WCR were ± 4 m s^{-1}. The location of the maximum updraft (in the primary wave, just downstream of the highest terrain) moved only 3 km over the 1 hour observation period.

Figure 7 (a and b) show results from a dual-Doppler synthesis completed in the strongest portion of the wave during the first pass. Figure 7a reveals that the strongest horizontal wind velocities occurred beneath the level of the UWKA about halfway down the slope of the mountain at approximately 1 km above ground level. The wave crest was just downwind of this position with broad, fairly laminar region of 2 to 4 m s^{-1} updraft (Figure 7b). Beneath the wave crest and downstream of the primary wave, there appeared significantly more turbulence, with some indication of flow separation above the valley floor.

Forty-five minutes after this time, during the third pass, there appears little change in the picture described above (Figure 8a and b). The amplitude of the primary wave has decreased somewhat (maximum vertical velocity is approximately 2.5 m s^{-1}). Also, the turbulence underneath the wave crest has decreased since the first pass. The flow separation that was more evident in the first pass with a suggestion of reversal of the horizontal flow underneath the crest has all but vanished by this time. Data from the 4th pass (not shown) approximately 10 minutes later offer further evidence of a transition from what appeared to have been a small rotor into a "normal" gravity wave feature.

4. SUMMARY

Observations were made of two wave systems on two different days during downwind of a mountain barrier in SE Wyoming. The observations were collected using an instrumented

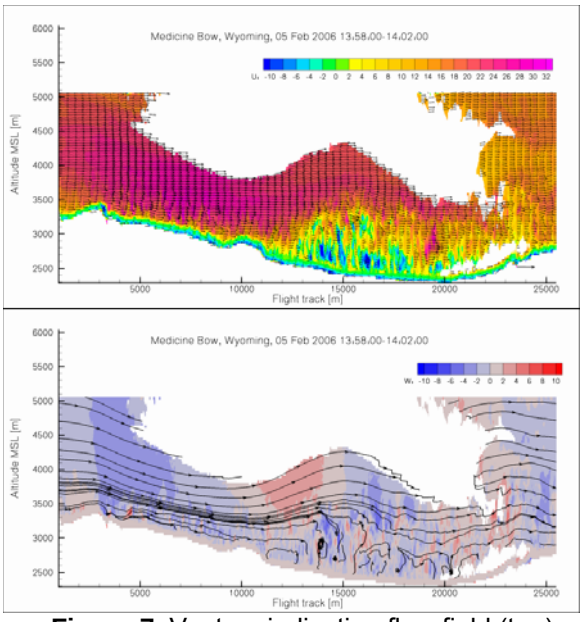

Figure 7: Vectors indicating flow field (top) derived from dual-Doppler sysnthesis of data data collected during the first pass on 5 Feb. The colorscale represents the magnitude of the horizontal wind. And streamlines (bottom) overlaid on the vertical velocity field, also from pass 1 on 5 Feb.

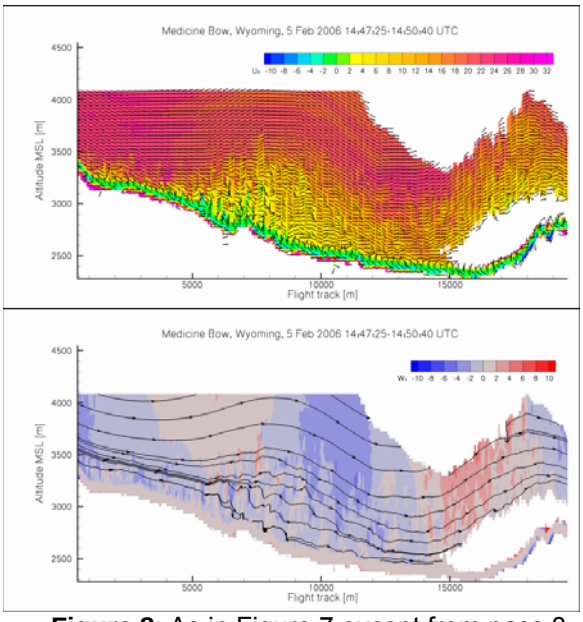

Figure 8: As in Figure 7 except from pass 3 on 5 Feb.

aircraft and an airborne Doppler radar. The radar provided two-dimensional cross-sections along the mean wind direction through the wave. Dual-Doppler synthesis provided an estimate of the along-plane velocity field beneath the aircraft. This allowed us to reconstruct a vertical slice revealing the two-dimensional kinematics within the wave system.

The case from 26 Jan appeared considerably stronger than that observed on 5 Feb. Maximum measured vertical winds were 2 to 3 times larger on 26 Jan, and maximum horizontal winds were 5 to 10 m s^{-1} larger (and confined to a region closer to the surface).

On both days there is some evidence of flow separation beneath the wave crest with a possible reversal of the near-surface flow indicated in the retrieved two-dimensional flow field. Unlike 5 Feb, the case of 26 Jan evolved rapidly, with a wave that apparently propagated upstream with time. Unfortunately the full evolution of the wave/rotor system was not observed on this day because following the third pass, the UWKA returned to base (due in part to the strong turbulence encountered in the last pass).

The 5 February case appeared much more stationary, however there still appeared a transition over the course of 1 hour from a rotor system with some hint of flow reversal near the surface to a more laminar flow throughout the depth of the wave.

Future work will focus on fully describing the meteorological conditions on the two days in order to better understand the thermodynamics and kinematics that led to the observed differences of the wave systems from the two cases. We will merge these observations from the NASA06 campaign with observations made during TREX06 using the UWKA and WCR. In particular, we will investigate how differences in orography, thermodynamics, and scales may affect the overall evolution of the wave/rotor system. Finally, we will engage in numerical modeling of these cases to further shed light on the above questions.

5. ACKOWLEDGEMENTS

This work was supported by the NSF under grants ATM-0742110. The NASA06 field campaign was sponsored by NASA grant, NCC5-578 (PIs Drs. B. Geerts, D. Leon, and J. Snider, University of Wyoming).

6. REFERENCES

Damiani, R., and S. Haimov, 2006: A high-resolution dual-Doppler technique fro fixed multiantenna airborne radar. *IEEE Trans. Geosci. and Rem. Sensing.,* **44**, 3475-3489

Leon, D., G. Vali, and M. Lothon, 2006: Dual-Doppler analysis in a single plane from an airborne platform. *J. Atmos. Ocean. Technol.,* **23**, 3-22.

Oolman, L., J. French, S. Haimov, D. Leon, and V. Grubisic, 2008: Observations of strong mountain waves in the lee of the Medicine Bow Mountains in SE Wyoming. *Preprint 13th Conf. Mtn. Meteorol.,* Am. Meteorol. Soc., Boston, MA.